The role of human antigen R (HuR) in modulating proliferation, senescence and radiosensitivity of skin cells

DAOJIANG YU[1], YAHUI FENG[1], ZHIQIANG JIANG[1], TAO YAN[1], KAI FANG[1], YUHONG SHI[1], JIE ZHANG[2] and SHUYU ZHANG[3-5]

[1]Department of Surgery, Second Affiliated Hospital of Chengdu Medical College, China National Nuclear Corporation 416 Hospital, Chengdu, Sichuan 610051; [2]Radiation Medicine Department of Institute of Preventive Medicine, Fourth Military Medical University, Xi'an, Shaanxi 710032; [3]Laboratory of Radiation Medicine, West China School of Basic Medical Sciences and Forensic Medicine; [4]Laboratory of Radiation Medicine, West China Second University Hospital, Sichuan University, Chengdu, Sichuan 610041; [5]Department of Nuclear Medicine, Second Affiliated Hospital of Chengdu Medical College, China National Nuclear Corporation 416 Hospital, Chengdu, Sichuan 610051, P.R. China

Received January 24, 2022; Accepted June 22, 2022

DOI: 10.3892/etm.2022.11503

Abstract. The skin is the largest outermost organ of the human body. It is vulnerable to various damages, such as ionizing radiation. Exploration of proliferation, senescence and radiosensitivity of skin cells contributes to the development of medical and cosmetic countermeasures against skin aging and toward injury protection. Human antigen R (HuR) is one of the most widely studied RNA-binding proteins and serves an important role in stabilization of mRNA and regulation of the expression of the target genes. To investigate the role of HuR in modulating proliferation, senescence and radiosensitivity of skin cells, the present study performed an *in vitro* study using lentivirus-mediated overexpression or silencing of HuR in human keratinocyte HaCaT cells and human skin fibroblast WS1 cells. The results indicated that overexpression of HuR promoted proliferation, whereas downregulation of HuR inhibited proliferation of HaCaT and WS1 cells. Overexpression of HuR reduced apoptosis and senescence in skin cells. RNA-Seq of skin cells with HuR overexpression or knockdown identified 77 mRNAs positively or negatively correlated with HuR expression levels. In addition, silencing of HuR induced a significant increase in radiogenic reactive oxygen species after irradiation. Overexpression of HuR increased radiotolerance of HaCaT and WS1 cells. RNA immunoprecipitation coupled with RNA-Seq identified 14 mRNAs interacting with HuR upon radiation exposure. Overall, the findings of the present study illustrated the key role of HuR in modulating proliferation, senescence and radiosensitivity of skin cells providing a new therapeutic strategy for cosmetic treatments and to combat skin injury.

Correspondence to: Professor Shuyu Zhang, Department of Nuclear Medicine, Second Affiliated Hospital of Chengdu Medical College, China National Nuclear Corporation 416 Hospital, No. 4, North 4th Section, Second Ring Road, Chengdu, Sichuan 610051, P.R. China
E-mail: zhang.shuyu@hotmail.com

Dr Jie Zhang, Radiation Medicine Department of Institute of Preventive Medicine, Fourth Military Medical University, 169 Changle Xi Road, Xi'an, Shaanxi 710032, P.R. China
E-mail: zhangjie78@fmmu.edu.cn

Key words: human antigen R, skin, proliferation, senescence, radiosensitivity

Introduction

Regulation of gene expression is a complex process that induces gene expression in the cells providing spatiotemporal response to changes in environmental conditions, which serve as the molecular basis of cellular differentiation, morphogenesis and ontogeny in the organism (1). This regulation can be carried out at multiple levels, including the gene, transcriptional, post-transcriptional, translational and post-translational levels (2-4). Post-translational protein modification is important and occurs in almost every protein during or after protein synthesis and can change the stability, structure, localization and function of the proteins (5). These modifications include ubiquitination, phosphorylation and dephosphorylation, glycosylation and deglycosylation, lipidation, methylation and acetylation (6,7). RNA-binding proteins (RBPs) are critical regulators of post-transcriptional gene regulation and a number of RBPs are modified after the translation to influence localization, stability and translation of the target mRNAs (5,8). Dysregulated post-translational modifications have been shown to influence pathological processes, such as cancer, neurodegenerative disorders and cardiovascular disease (9). RBPs exert significant control over numerous cellular functions and thus represent a popular area of investigations by scientists. Recent developments in experimental identification of RBPs significantly expanded the number of known RBPs. Although RBPs serve a crucial role in post-transcriptional regulation of gene expression, relatively few RBPs have been studied systematically (10,11).

Human antigen R (HuR; also known as HuA or ELAVL1) is one of the most extensively studied RBPs and serves an important role in the stabilization of mRNAs containing AU-rich elements (AREs) and regulation of the expression of the target genes (12). When cells are under normal conditions, HuR is mainly located in the nucleus and is in an inactivated state. When cells encounter certain pathological environments, such as hypoxia, radiation damage and cytokine stimuli, HuR translocates from the nucleus to the cytoplasm by binding and interacting with various 3'-UTR AREs (8,12-14). Thus, HuR can protect mRNAs from nuclease degradation in the process of translocation from the nucleus to the cytoplasm and increase the stability of mRNAs. HuR has been shown to serve important roles in tumorigenesis and malignant transformation and to regulate oncogenes, the cell cycle, apoptosis, inflammatory factors, invasion, metastasis and related molecules by binding to the target genes (15-18). In addition, several studies have shown that HuR contributes to the development of resistance to chemotherapy in multiple types of cancer (14,19,20). c-Myc, p53, cyclin D1, cyclin A, survivin, Bcl-2, cyclooxygenase (COX)-2, VEGF and MMP-9 have been identified as the downstream targets of HuR depending on specific cell type (21).

The skin is the largest outermost organ of the human body. The primary role of the skin is to serve as a physical barrier, protecting our bodies from potential assault by foreign organisms or toxic substances. HuR is known to be modulated by mitogenic and stress-causing agents, including UV radiation (22). Stress-induced modulation of HuR activity may be achieved by phosphorylation resulting in its translocation to the cytoplasm. HuR binds to COX-2 mRNA in a constitutive manner and forced overexpression of an HuR-GFP construct stabilizes COX-2 mRNA in unstimulated HaCaT cells (23). Given the importance of HuR in gene regulation, the aim of the present study was to elucidate further the role and regulatory mechanisms of HuR in proliferation, senescence and radiosensitivity of the skin

Materials and methods

Vectors and viruses. In the present study, the third generation of four-plasmid lentivirus vector system was used. The lentiviral vector system was composed of four plasmids: The expression plasmid and three packaging vectors, including 1.5 μg pMDLg-pRRE, 1.5 μg pMD2.G and 1.5 μg pRSV-Rev Virus packaging helper plasmids. Lentiviral vectors and packaging vectors were transfected into 293T cells (Wuhan GeneCreate Biological Engineering Co., Ltd.). 293T cells were seeded with DMEM (HyClone; Cytiva) supplemented with 10% fetal bovine serum (FBS; cat. no. 04-001-1A; Biological Industries) and cultured in a 37˚C incubator with a 6-well plate of 2 ml/well. When the cell density reached 70-80%, it was used for transfection. The cells were cultured in serum-free medium before transfection. 2 μg expression plasmid, 1.5 μg PMDLG-PRRE, 1.5 μg PMD2.g and 1.5 μg PRSV-Rev virus packing assistant plasmid were diluted in 500 μl serum-free medium. Lipofectamine® 2000 (15 μl; Invitrogen; Thermo Fisher Scientific, Inc.) was diluted with 500 μl serum-free medium. After standing for 5 min, The DNA solution was mixed with Lipofectamine® 2000 solution and stood for 20 min at room temperature. Serum-free medium (1 ml) was taken from the 6-well plate and 1 ml plasmid and Lipofectamine® 2000 were dropped into the 6-well plate at 37˚C and 5% CO_2 for 8 h. Following transfection, the culture medium was exchanged with DMEM (HyClone; Cytiva) supplemented with 10% fetal bovine serum (FBS; cat. no. 04-001-1A; Biological Industries). After 48 h, the supernatant containing the retroviral particles was collected and then concentrated by centrifugation at 4,000 x g for 10 min at 4˚C. The cell supernatant was filtered by a 0.45 μm filter into a 50 ml ultrafast centrifuge tube and 5X PEG8000 was added to precipitate at 4˚C overnight. After centrifugation at 7,000 x g, the supernatant was discarded and the precipitation was redissolved with 10 ml PBS. The viral supernatants were added to the upper layer of 20% sucrose solution, centrifuged at 20,000 x g for 2 h and 4˚C. The precipitate was suspended with 1 ml PBS and filtered by a 0.22 μm filter for sterilization. The virus suspension was separated into 50 μl and stored at -80˚C. A total of $1x10^5$ cells/well were transduced with viral supernatants. The cells were collected for subsequent experiments after being cultured in fresh medium for 48 h at 37˚C.

HuR overexpression and short hairpin (sh)RNA lentiviruses. The human HuR coding region was amplified by polymerase chain reaction (PCR) using a primer pair specific to HuR. The fragments were inserted into the lentiviral expression vectors (LV-HuR) and then packaged into viral particles. The negative control lentiviral (LV-NC) was constructed by not inserting any sequences. Lentivirus silencing HuR through shRNAs were obtained from Hanbio Biotechnology (containing RFP). The targeting sequences of shRNA control (sh-NC) and four shRNA targeting HuR (sh-HuR-1, sh-HuR-2, sh-HuR-3 and sh-HuR-4) are listed in Table SI.

Cell culture and transfection. Human keratinocyte HaCaT (cat. no. iCell-h006, iCell Bioscience Inc.) and human skin fibroblast WS1 (cat. no. CRL-1502T; ATCC) cells were maintained in DMEM supplemented with 10% FBS and 100 U/ml penicillin-streptomycin at 37˚C and a 5% CO_2 atmosphere. For transfection, cells were transfected by Lipofectamine® 2000 (Invitrogen; Thermo Fisher Scientific, Inc.) with viral particles. Cells were exposed to a single dose (20 Gy) of X-rays using the linear accelerator (RadSource) at a dose rate of 1.15 Gy/min. The HaCaT cell line was obtained from iCell Bioscience Inc. DNA was extracted with Axygen genome extraction kit (cat. no. AP-GX-250; Axygen® AxyPrep DNA Gel Extraction Kit; Corning, Inc.) and amplified with 21-str amplification scheme. STR loci and sex gene Amelogenin were detected on an ABI 3730XL genetic analyzer (Applied Biosytems; Thermo Fisher Scientific, Inc.). The results showed that the cell line was completely matched by DNA typing in cell line retrieval and the cell name was HACAT and the cell number was 771 according to DSMZ database. No multiple alleles were found in this cell line.

Reverse transcription-quantitative (RT-q) PCR. After cells reached 90% confluence, total RNA was extracted using TRIzol® reagent (cat. no. 15596018; Thermo Fisher Scientific, Inc.) in accordance with the manufacturer's instructions. RNA was reverse transcribed using a reverse transcription

kit (cat. no. K1691; RevertAid RT Reverse Transcription kit; Thermo Fisher Scientific, Inc.) under 42˚C for 60 min and 70˚C for 5 min. The mRNA level of *HuR* gene in each sample was measured by RT-PCR. The reaction was performed at 37˚C for 15 min followed by 85˚C for 5 sec. cDNA was amplified via qPCR with TB Green dye (cat. no. RR420S; Takara Bio, Inc.) on a Prism 7500 RT-PCR machine (Applied Biosystems; Thermo-Fisher Scientific, Inc.). The thermocycling conditions included an initial denaturation step of 95˚C for 60 sec, followed by 40 cycles of amplification at 95˚C for 15 sec and then annealing at 60˚C for 30 sec. *GAPDH* was used as an endogenous standard. The relative amount of target genes was carried out according to the $2^{-\Delta\Delta Cq}$ algorithm (24). The experiments were repeated three times (HUR: Forward Primer 5'-GGGTGACATCGGGAGAACG-3', Reverse Primer 5'-CTGAACAGGCTTCGTAACTCAT-3'; GAPDH: Forward Primer 5'-GGAGCGAGATCCCTCCAAAAT-3', Reverse Primer 5'-GGCTGTTGTCATACTTCTCATGG-3').

Western blotting analysis. The cells were lysed in lysis buffer (Promega Corporation) and centrifuged at 4˚C, 12,000 x g for 10 min. The supernatant was collected and subjected to western blotting. Protein concentration was subsequently measured using a BCA Protein Assay kit (cat. no. P0012; Beyotime Institute of Biotechnology). Protein (50 μg) from each lysate was fractionated by 10% SDS-PAGE. The samples were electrophoresed for 2 h and transferred onto polyvinylidene difluoride membranes (MilliporeSigma). After being blocked with 5% BSA in TBS-0.1% Tween-20 (TBST) for 1 h at room temperature, the membranes were blotted with HuR (Abcam; cat. no. ab220342) or α-Tubulin (Beyotime Institute of Biotechnology; cat. no. AF0001) primary antibodies at 1:1,000 dilutions. The membranes were then incubated with the appropriate horseradish peroxidase-coupled secondary antibody (Beyotime Institute of Biotechnology; cat. no. A0277) at a 1:2,000 dilution for 1 h at room temperature. After the membranes were washed with TBST, the blots were incubated with enhanced chemiluminescence (ECL) stable peroxide solution (Beyotime Institute of Biotechnology). All blots were visualized using a FluoroChem MI imaging system (Alpha Innotech Corporation) at room temperature. Densitometry was performed using ImageJ v1.8.0-172 software (National Institutes of Health).

Cell viability assay. Cell viability was evaluated using the Cell Counting Kit-8 (CCK-8; Dojindo Laboratories, Inc.) assay. HaCaT and WS1 cells were plated in 96-well plates and cultured for 12 h at 37˚C in a CO_2 incubator. The cells were transfected with LV-NC, LV-HuR, sh-NC, sh-HuR-1 and sh-HuR-2 viral particles. After treatment for 24 and 48 h at 37˚C in a CO_2 incubator, the cells were then incubated with 10 μl CCK-8 for 4 h. Then the optical density (OD) at 450 nm was measured using a Microplate Reader (Bio-Rad Laboratories, Inc.). The viability index was calculated as experimental OD value/control OD value. Three independent experiments were performed in quadruplicate.

EdU assay. The proliferation of HaCaT and WS1 cells transfected with different viral particles was determined by 5-Ethynyl-2'-deoxyuridine (EdU) assay kit. Cells were pre-infected with LV-NC, LV-HuR, sh-NC, sh-HuR-1 and sh-HuR-2 viral particles for 24 h at 37˚C in a CO_2 incubator before receiving sham or 20 Gy X-ray irradiation, after irradiation for 48 h at 37˚C in a CO_2 incubator, cells were labeled with 50 μM EdU (Guangzhou RiboBio Co., Ltd.) for 4 h at 37˚C in a CO_2 incubator. Then, the cells were fixed with 4% formaldehyde for 15 min at room temperature and treated with 0.5% Triton X-100 for 20 min at room temperature. The cells were washed with PBS for three times and treated with 100 μl of 1X ApolloR (EdU; Guangzhou RiboBio Co., Ltd.) reaction cocktail in the dark at room temperature for 30 min. Subsequently, the DNA of each well of cells were stained with 4',6-diamidino-2-phenylindole dihydrochloride (DAPI; MilliporeSigma) for 30 min at room temperature and observed under a fluorescence microscope (Olympus Corporation).

Clonogenic assay. For standard clonogenic assays, cells were re-suspended and seeded into six-well plates at 200 cells/well, cells were pre-infected with LV-NC, LV-HuR, sh-NC, sh-HuR-1 and sh-HuR-2 viral particles 24 h at 37˚C in a CO_2 incubator before receiving sham or 20 Gy X-ray irradiation. The cells were grown from 7-10 days to allow for colony formation and were subsequently fixed and stained using crystal violet. Colonies consisting of >50 cells were counted as a clone.

Apoptosis analysis. Apoptosis was measured using propidium iodide (PI)/Annexin-V double staining following manufacturer's instructions (BD Biosciences). Cells were pre-infected with LV-NC, LV-HuR, sh-NC, sh-HuR-1 and sh-HuR-2 viral particles 24 h at 37˚C in a CO_2 incubator before receiving sham or 20 Gy X-ray irradiation. After irradiation for 48 h, HaCaT and WS1 cells were harvested and apoptotic fractions were measured using flow cytometry (Beckman Coulter, Inc.). The Annexin-V+/PI- cells are early in the apoptotic process, the Annexin-V+/PI+ cells indicating late apoptosis. The percentage of both types of cells was counted. To compute the percentage of apoptotic cells, a flow cytometer (FACSCalibur; BD Biosciences) with ModFit's LT v.3.0 software (BD Diagnostics) was used for data analysis.

Cell senescence staining. The cell senescence of HaCaT and WS1 cells transfected with different viral particles was determined by β-galactosidase staining. After the cells were transfected with LV-NC, LV-HuR, sh-NC, sh-HuR-1 and sh-HuR-2 viral particles for 24 h at 37˚C in a CO_2 incubator. The cell senescence staining was performed according to the β-galactosidase staining kit (Beyotime Institute of Biotechnology).

Cell senescence assay. HaCaT and WS1 cells were fixed in 2% formaldehyde/0.2% glutaraldehyde for 5 min at room temperature. β-Galactosidase staining solution containing X-gal (cat. no. C0602; Beyotime Institute of Biotechnology) was added after rinsing with PBS. The cells were then incubated for 6-10 h in a 37˚C incubator without CO_2. Senescent cells (stained blue) were observed and images were captured using light microscopy (Olympus Corporation; magnification, x10) and positive staining areas were calculated by determining the percentage of SA-β-gal$^+$ cells in five random fields in each of the three wells.

Reactive oxygen species (ROS) generation assay. ROS levels after irradiation were determined using the ROS assay kit (Beyotime Institute of Biotechnology). HaCaT and WS1 cells were pre-infected with sh-NC, sh-HuR-1 and sh-HuR-2 viral particles 24 h at 37˚C in a CO_2 incubator before receiving 20 Gy X-ray irradiation. After irradiation for 24 h, cells were labeled with 10 μM 2,7-dichlorofluorescein diacetate (DCFH-DA) at 37˚C for 30 min. Then, the cells were fixed with 4% formaldehyde for 15 min at room temperature and washed with PBS for three times, after then treated with 5 μg/ml Hoechst 33258 (Beyotime Institute of Biotechnology) for 30 min and observed under a fluorescence microscope (PerkinElmer, Inc.).

Sample preparation for RNA-seq. Total RNA was extracted from HaCaT cells infected with LV-NC, LV-HuR, sh-NC or sh-HuR-1 lentiviruses (n=3) using TRIzol® reagent (Thermo Fisher Scientific, Inc.). For RNA high-throughput sequencing, RNA libraries were created from each group using the NEBNext Ultra Directional RNA Library preparation kit from Illumina, Inc. The main steps in the workflow involved the removal of ribosomal RNA, the fragmentation of total RNA, reverse transcription and second-strand complementary DNA (cDNA) synthesis, end repair, dA tailing and adaptor ligation. The products of these reactions were purified and enriched by polymerase chain reaction to create the final cDNA library. The libraries were then sequenced using an Illumina HiSeq2500 (paired-end sequencing; Illumina, Inc.).

RNA-seq data acquisition and quality control. The RNA sequence row data was obtained by RNA-seq on the Illumina platform. Then, the reads were clipped and trimmed to avoid low-quality data using Trim Galore (http://www.bioinformatics.babraham.ac.uk/projects/trim_galore/). Trimmed sequence files underwent quality control analysis using FastQC (http://www.bioinformatics.babraham.ac.uk/projects/fastqc/). The present study utilized several parameters to evaluate the read quality, including the number of the reads, guanine-cytosine (GC) contents and average length of the reads.

Differential expression analysis of genes. For the analysis of differentially expressed genes, the clean data for each sample were aligned to the rat reference genome (ftp://ftp.ensembl.org/pub/release-83/fasta/rattus_norvegicus/dna/) using TopHat (version 2.0.10) software (http://ccb.jhu.edu/software/tophat/index.shtml). The alignment files were assembled using Cufflinks (http://cole-trapnell-lab.github.io/cufflinks/) and the StringTie software (http://ccb.jhu.edu/software/stringtie/) based on the location of the known transcript and the transcripts of all samples were assembled again using Cuffmerge (http://cole-trapnell-lab.github.io/cufflinks/cuffmerge/index.html). The differential gene expressed values of each sample were normalized using the fragments per kilobase of transcript per million fragments mapped. The differential expression levels were calculated and the statistical significance of detected genes evaluated. Genes were considered as significantly differentially expressed with false discovery rates (FDRs) ≤0.05 and fold-changes ≥1.0.

Functional enrichment analysis. The database for annotation, visualization and integrated discovery (DAVID; http://david.abcc.ncifcrf.gov/) was used, which leveraged the Gene Ontology (GO) to determine the most functional annotation and classification of significant differently expressed genes and DEL targets. To demonstrate GO or molecular pathway enrichment, DAVID calculates a modified Fisher exact P-value. P-value <0.05 was considered to be strongly enriched in the annotation category. In addition, the present study used the Kyoto Encyclopedia of Genes and Genomes (KEGG) database (http://www.genome.ad.jp/kegg/) to analyze the roles of differently expressed genes and DEL targets in the pathways.

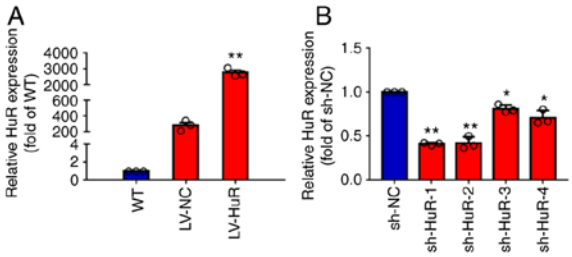

Figure 1. The overexpression and silencing of HuR in skin cells. Reverse transcription-quantitative PCR analysis of (A) the overexpression efficiency of lentiviral vectors and (B) the silencing efficiency of four shRNA targeting HuR gene (shRNA-HuR). *P<0.05, **P<0.01. HuR, Human antigen R; sh, short hairpin.

RNA immunoprecipitation (RIP) and sequencing. RIP was performed as described previously (21). This radiation dose (5 Gy X-ray) was selected because WS1 cells are more sensitive to radiation. The doses in cell studies were the same as previous publications of others and our own (25,26). In short, WS1 cells were washed with PBS and harvested by adding 150 ml of immunoprecipitation buffer (10 mM Tris-HCl, pH 7.4, 50 mM NaCl, 0.5 mM EDTA, 1 mM phenylmethanesulfonylfluoride and 1% Triton X-100). After the cells were sonicated (25 KHz, 5 sec/time) for 2 min on ice, insoluble material was removed by centrifugation at 2,500 x g, 15 min, 4˚C. Supernatants were collected and pre-cleared by agarose-coupled protein A. The agarose beads were removed by centrifugation at 2,500 x g, 5 min, 4˚C. HuR (CST; cat. no. MA1-167) antibody and GAPDH (Abcam; cat. no. ab181602;) antibody were added to the supernatants (1:100 ratio) and the reaction was incubated at 4˚C overnight with gentle rotation. Agarose-coupled protein A (50 μl) were added to capture the antibody-protein complexes by rotating for 2 h at 4˚C. The supernatants were then removed by centrifuging at 2,000 x g and 4˚C for 5 min. RNA was extracted using TRIzol® following the manufacturer's instructions (Thermo Fisher Scientific, Inc.). rRNAs were removed from the immunoprecipitated RNA and input RNA samples by using Ribo-Zero rRNA Removal kit (Illumina, Inc.). RNA libraries were constructed by using rRNA-depleted RNAs with TruSeq Stranded Total RNA Library Prep kit (Illumina, Inc.) according to the manufacturer's instructions. Libraries were controlled for quality and quantified using the BioAnalyzer 2100 system (Agilent Technologies, Inc.). Libraries (10 pM) were denatured as single-stranded DNA molecules, captured on Illumina flow cells, amplified *in situ* as clusters and finally sequenced for 150 cycles on an Illumina HiSeq Sequencer according to the manufacturer's instructions by CloudSeq.

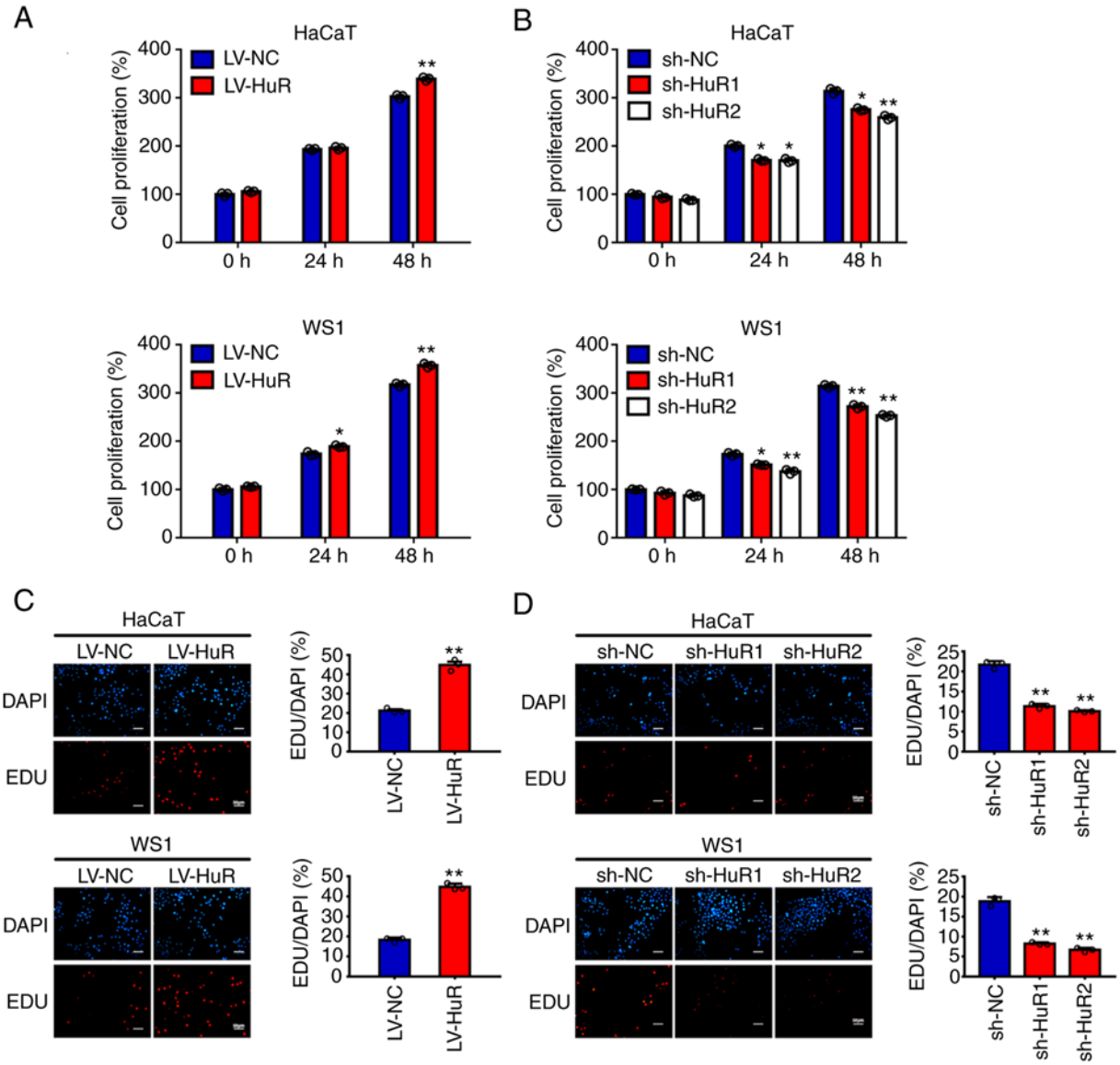

Figure 2. Overexpression and silencing of HuR affected the cell proliferation of HaCaT and WS1 cells. The cell viability of (A) overexpression and (B) silencing of HuR on HaCaT and WS1 was measured by CCK-8 assay. EdU-based staining of HaCaT and WS1 after (C) overexpression and (D) silencing of HuR. Scale bar, 100 μm. *P<0.05, **P<0.01. HuR, Human antigen R; sh, short hairpin; NC, negative control; LV, lentiviral.

Statistical analysis. The data were evaluated using either unpaired two-sided Student's t-tests or one-way analysis of variance to determine statistical significance after confirming that the data met appropriate assumptions. For all experiments, three biological replicates were analyzed for each condition and presented as the mean ± standard error of the mean. Differences between two groups were determined using a paired Student's t-test and differences among >2 groups were analyzed by one-way analysis of variance and Tukey post hoc tests. Statistical analysis was performed using Prism 7 software (GraphPad Software, Inc.). Data are expressed as mean ± standard error of the mean. P<0.05 was considered to indicate a statistically significant difference.

Results

Overexpression and silencing of HuR in skin cells. To test the overexpression of LV-HuR, the present study measured HuR expression by RT-qPCR and western blotting. The results showed that the expression of HuR mRNA in LV-HuR cells was significantly higher compared with that in LV-NC cells (Fig. 1A). In addition, the silencing effect of sh-NC and four shRNAs targeting HuR (designated sh-HuR-1, sh-HuR-2, sh-HuR-3 and sh-HuR-4) was also tested. The results showed that four sh-HuRs significantly reduced the expression of HuR and sh-HuR-1 and sh-HuR-2 had the strongest silencing effect (Fig. 1A); subsequent experiments were performed using these two sh-HuR vectors.

The effects of HuR on proliferation and apoptosis of skin cells. Initially, the present study investigated the effect of HuR on the proliferation of skin cells by a CCK-8 assay. The results showed that overexpression of HuR promoted the growth of HaCaT and WS1 cells (Fig. 2A) and silencing HuR inhibited the growth of these cells (Fig. 2B). Then, EdU staining was used to confirm the role of HuR in the proliferation of skin

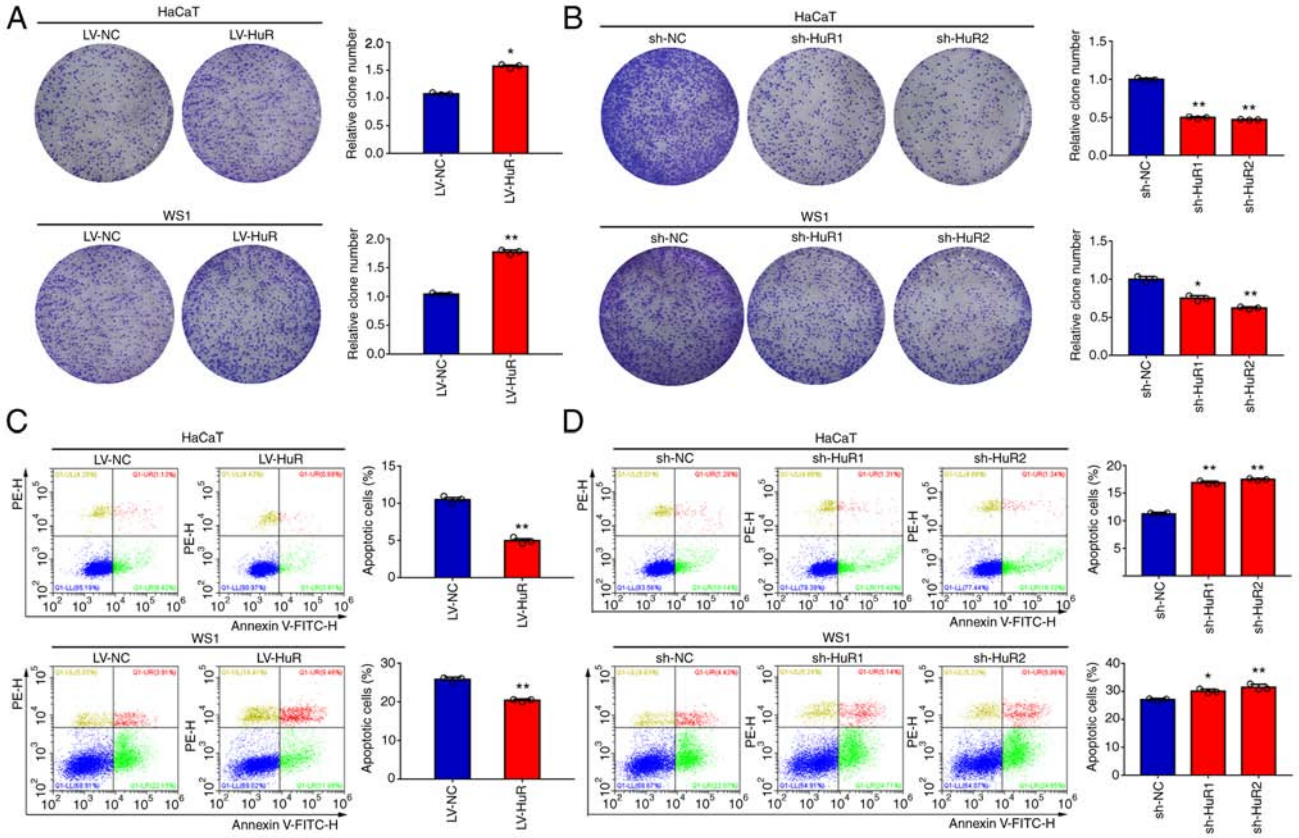

Figure 3. Overexpression and silencing of HuR modulates the cell clonogenic survival and apoptosis of HaCaT and WS1. Clonogenic survival staining of HaCaT and WS1 after (A) overexpression and (B) silencing of HuR. Flow cytometry measured cell apoptosis of HaCaT and WS1 after (C) overexpression and (D) silencing of HuR. *P<0.05, **P<0.01. HuR, Human antigen R; sh, short hairpin; NC, negative control; LV, lentiviral.

cells. The results also showed a positive association of HuR with the percentage of EdU-positive HaCaT and WS1 cells (Fig. 2C and D). The results of a colony formation assay showed that clonogenicity of HaCaT and WS1 cells was significantly increased or reduced when HuR was overexpressed or silenced, respectively (Fig. 3A and B). The results of a flow cytometry-based apoptosis assay showed that overexpression of HuR reduced apoptosis of HaCaT and WS1 cells (Fig. 3C). Conversely, downregulation of HuR increased apoptosis in the two skin cell lines (Fig. 3D).

The effects of HuR on skin cell senescence. Temporal and environmental aging influences skin structure and functions, including the skin barrier and elastic and mechanical properties of cutaneous tissue associated with alterations of biomechanical properties of skin cells (27). Thus, the present study evaluated the effect of HuR expression levels on HaCaT and WS1 cell senescence. Cellular senescence was evaluated by β-galactosidase staining (28). The results of senescence staining in Fig. 4A showed that senescence of HuR-overexpressing WS1 and HaCaT cells was reduced by 50%. The results of Fig. 4B indicated that senescence was increased by 60% in the cells with silenced HuR. These results showed that overexpression of HuR reduced senescence of HaCaT and WS1 cells and that HuR silencing increased senescence.

HuR modulated the expression of mRNAs in skin cells. Since HuR influences the stability of mRNAs (7,8), the present study sought to explore the landscape of HuR-influenced mRNAs in skin cells. RNA-Seq was performed in WS1 cells with HuR overexpression or downregulation. The RNA-Seq data are accessible from the GEO database (accession number GSE161811). The results showed that comparison with the control group (LV-NC) detected 2947 differentially expressed genes in the overexpression group (LV-HuR; Fig. 5A and B), including 1,449 upregulated genes and 1,498 downregulated mRNAs. A total of 134 differentially expressed genes were detected in the silenced group (sh-HuR vs. sh-NC), including 99 upregulated and 35 downregulated genes (Fig. 5C and D). Combined sequencing data indicated that HuR positively regulated 52 mRNAs and negatively regulated 25 mRNAs (Fig. S1). These mRNAs included CALB2, INHBA, ACSS2, OLFM4 and TMPRSS11E.

The effect of HuR on skin cell radiosensitivity. Radiation-induced skin injury is a common complication after radiation accidents, tumor radiation therapy and bone marrow transplantation pretreatment (29,30). ROS produced by ionizing radiation in the skin are an important cause of skin injury (31,32). The present study explored the effect of HuR on intracellular ROS levels after radiation and the results showed that the level of ROS in the sh-HuR group was significantly increased after 20 Gy X-ray irradiation (Fig. 6A). In addition, we investigated the effects of HuR on the proliferation and apoptosis of HaCaT and WS1 cells after irradiation. The results of EdU staining showed that overexpression of HuR

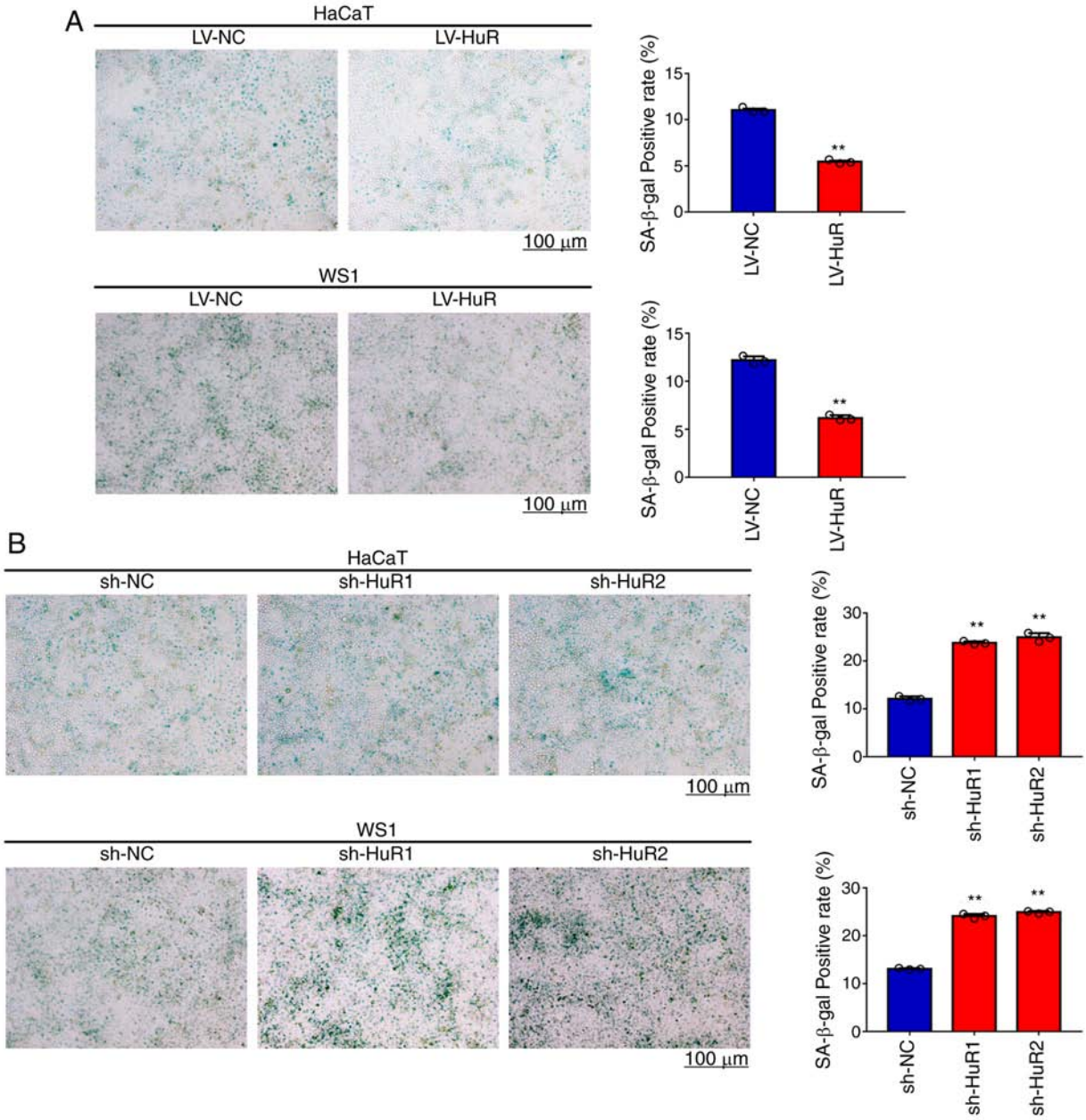

Figure 4. Overexpression and silencing of HuR modulates the cell senescence of skin cells. (A) β-galactosidase staining of HaCaT and WS1 cells after overexpression of HuR. (B) β-galactosidase staining of HaCaT and WS1 cells after silencing of HuR. Representative images of staining and calculated positive cell percentage are shown. Scale bar, 100 μm. **P<0.01. HuR, Human antigen R; sh, short hairpin; NC, negative control; LV, lentiviral.

promoted cell proliferation after 20 Gy X-ray irradiation (Fig. 6B) and downregulation of HuR enhanced inhibition of cell proliferation after irradiation (Fig. 6C). The results of a colony formation assay showed that overexpression of HuR significantly increased cell survival after X-ray irradiation at 20 Gy (Fig. 6D); however, downregulation of HuR significantly reduced cell survival after irradiation (Fig. 6E). The results of a cellular apoptosis assay showed that overexpression of HuR reduced apoptosis of HaCaT and WS1 cells after X-ray irradiation at 20 Gy (Fig. 6F) and HuR silencing increased apoptosis after irradiation (Fig. 6G). Overall, these results indicated that HuR modulated radiosensitivity of skin cells *in vitro*.

Characterization of HuR-interacting mRNAs after irradiation. The present study used RIP combined with RNA-Seq to detect changes in the HuR-binding sequence and expression profile of WS1 cells after 0 or 5 Gy irradiation (Fig. 7A). The RNA-Seq data are accessible from the GEO database (accession number GSE111823). The results indicated the lack of significant changes in the binding locations (Fig. 7C). Hundreds of HuR-binding sites were changed after 5 Gy irradiation (Fig. 7B). Combined data of RIP-Seq and RNA-Seq indicated that 14 mRNAs were associated with changes in HuR binding and expression after irradiation (Fig. 7D), indicating that the abundance of these mRNAs may be modulated by HuR binding (Figs. S2 and S3). For example, the levels of NLRP10, SERPINE1 and CLCA2 mRNAs were increased in WS1 cells after 5 Gy irradiation. NLRP10 is expressed at high levels in the skin and contributes to cell-autonomous responses against invasive bacteria. HUR

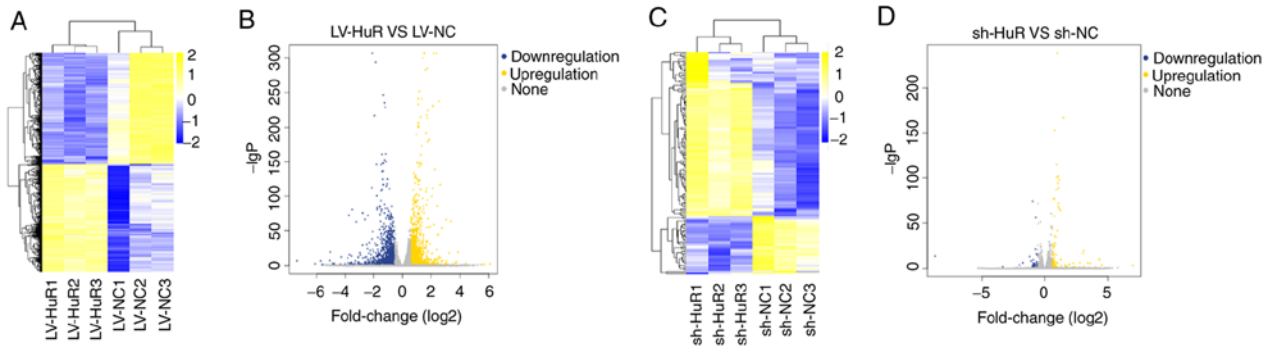

Figure 5. The effect of HuR on downstream mRNAs by RNA-Seq. (A) The heatmap of significant differently expressed mRNA (LV-HuR vs. LV-NC group). (B) Volcano plot of the significant differently expressed mRNA (LV-HuR vs. LV-NC group). (C) The heatmap of significant differently expressed mRNA (sh-HuR vs. sh-NC group). (D) Volcano plot of the significant differently expressed mRNA (sh-HuR vs. sh-NC group). HuR, Human antigen R; sh, short hairpin; NC, negative control; LV, lentiviral.

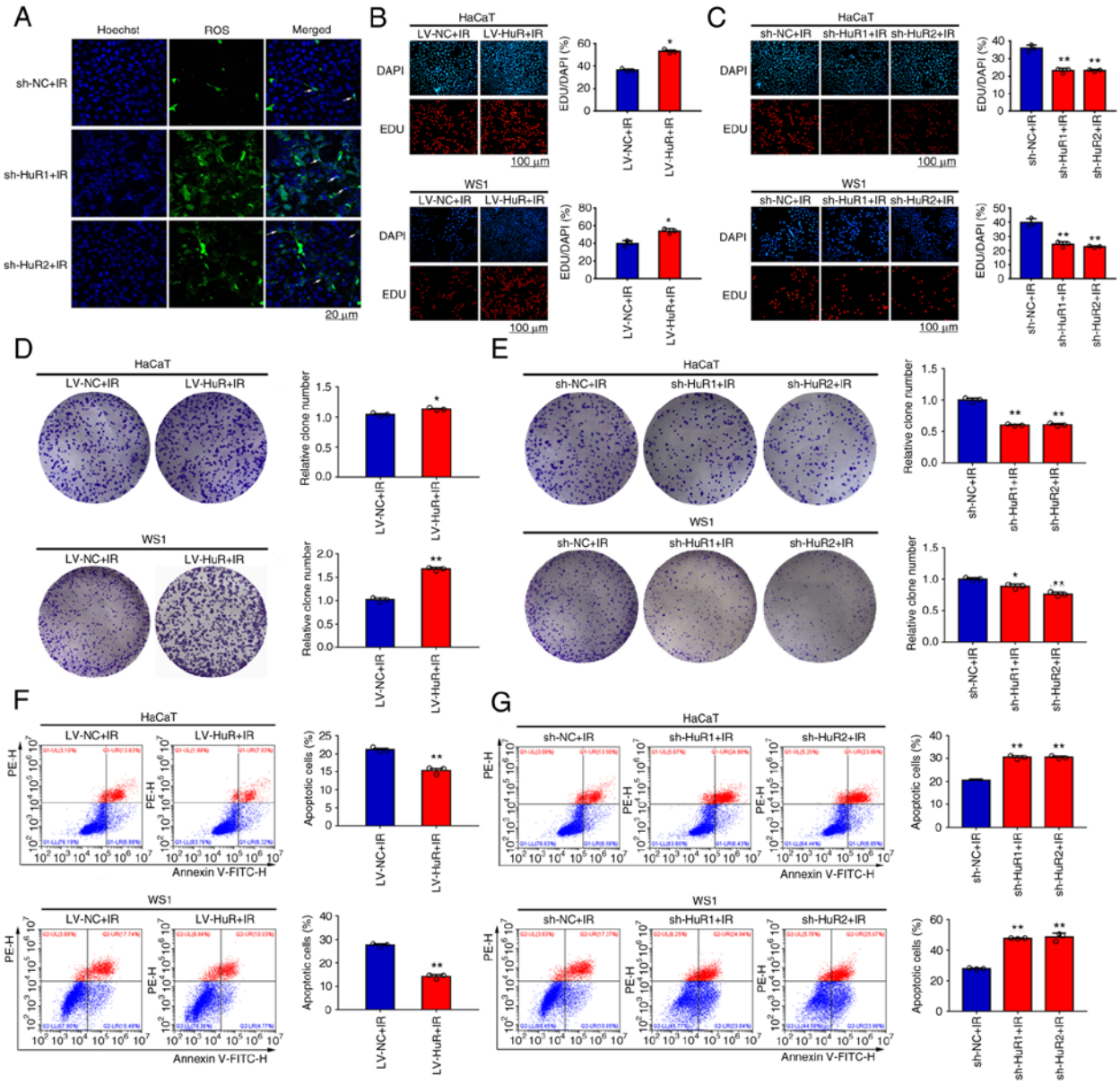

Figure 6. Overexpression and silencing of HuR affected the cell radiosensitivity of skin cells. (A) The ROS of HaCaT cells pre-infected with sh-NC, sh-HuR-1 or sh-HuR-2 viral after receiving 20 Gy X-ray irradiation. Scale bar, 20 μm. EdU staining of HaCaT and WS1 after (B) overexpression and (C) silencing of HuR with 20 Gy X-ray irradiation. Scale bar, 100 μm. Clonogenic survival staining of HaCaT and WS1 after (D) overexpression and (E) silencing of HuR with 20 Gy X-ray irradiation. Flow Cytometry measured cell apoptosis of HaCaT and WS1 after (F) overexpression and (G) silencing of HuR with 20 Gy X-ray irradiation. *P<0.05, **P<0.01. HuR, Human antigen R; ROS, reactive oxygen species; sh, short hairpin; NC, negative control; LV, lentiviral.

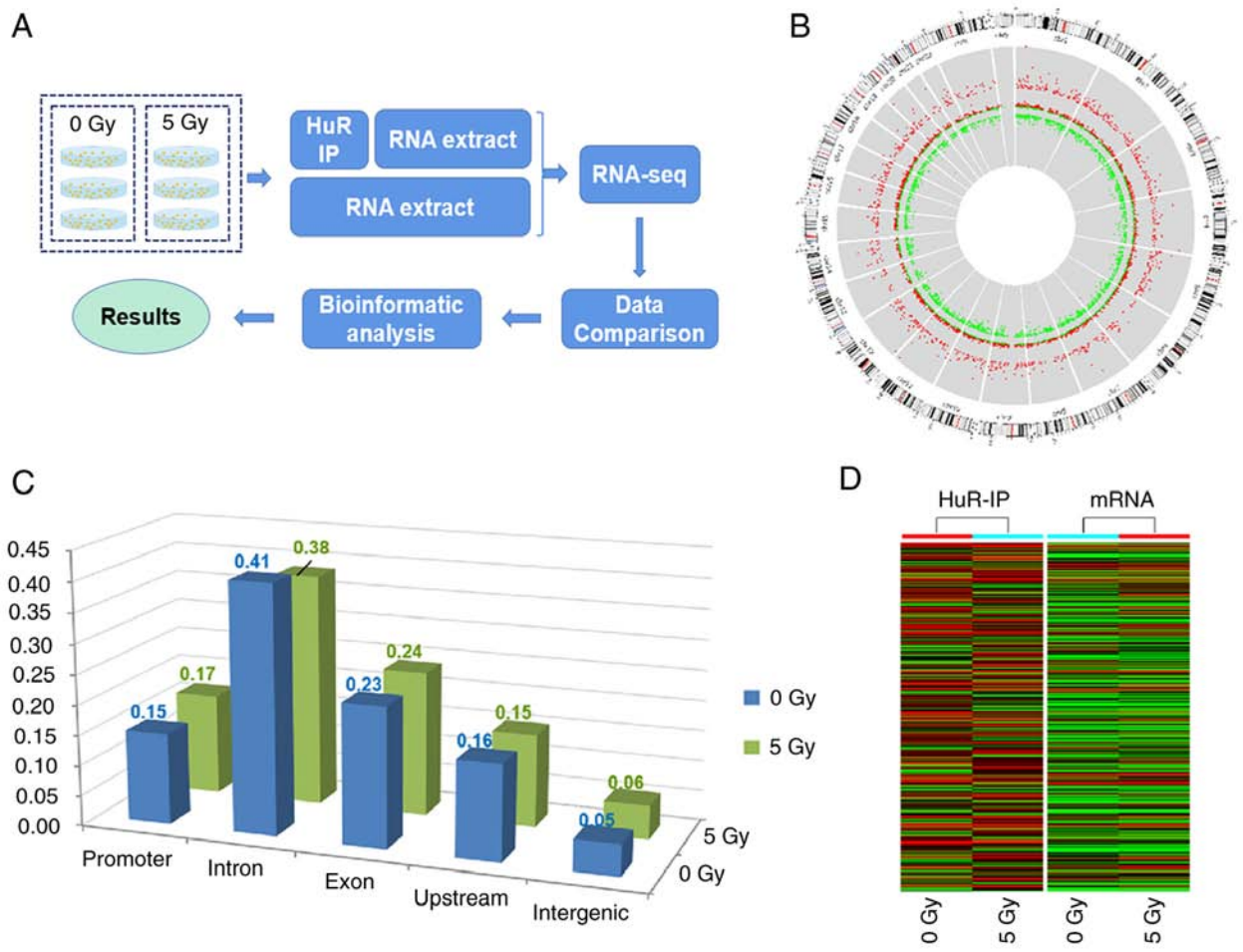

Figure 7. RIP-seq to screen HuR-interacted mRNAs upon radiation. (A) Experimental design of the HuR RIP-seq analysis. (B) Differentially gene regions in human chromosomes. Red and green bars represent upregulated and downregulated sites, respectively. (C) Percentage of the location of gene regions. (D) Heatmap of HuR RIP genes and corresponding mRNA after 0 or 5 Gy X-ray irradiation. RIP-seq, RNA immunoprecipitation and sequencing; HuR, Human antigen R; ROS, reactive oxygen species; sh, short hairpin; NC, negative control; LV, lentiviral.

exerted its influence through wide spectrum targets, which was consistent with its behavior in other types of cells. These genes were explored by RIP-Seq and RNA Seq in the present study. However, which one could be the exact target for HUR that leads to cell proliferation, senescence and radiosensitivity needs to be further studied.

Discussion

HuR is an RNA-binding protein that recognizes U/AU-rich elements in diverse RNAs and post-transcriptionally regulates the fate of target RNAs. HuR regulates cellular responses to differentiation, senescence, inflammatory factors and immune stimuli by tightly controlling the post-transcriptional fate of specific mRNAs (33,34). HuR is expressed at high levels in a number of types of cancers and is believed to promote tumorigenesis by interacting with mRNAs encoding proteins implicated in cell proliferation and survival, angiogenesis, invasion and metastasis (23). For example, HuR serves pro-proliferative and anti-apoptotic roles in colorectal cancer cells (5). In the present study, the role of HuR in modulating proliferation and senescence of skin cells was explored using HuR overexpression and silencing. Consistent with previous reports in other cell lines, HuR facilitated the proliferation of skin cells and inhibited their senescence, suggesting a new therapeutic strategy for cosmetic treatments and to combat skin injury.

HuR has been shown to associate with numerous transcripts, including coding and noncoding transcripts, and controls their splicing, localization, stability and translation (16). HuR is predominantly nuclear in unstimulated cells and shuttles to the cytoplasm in response to various stimuli, including stress signals and mitogens (5). HuR stabilizes a large subset of target mRNAs, including mRNAs implicated in various pathologies, particularly cancer and inflammation (16). Known HuR-regulated mRNAs include cyclin family proteins (A2, B1, E1 and D1), cyclin-dependent kinase inhibitor p21, inducible nitric oxide synthase, granulocyte-macrophage colony-stimulating factor, murine double minute 2, VEGF, TGF-β, TNF-α, Bcl-2, COX-2, p53, Toll-like receptor 4, MMP-9 and MAPK (35). In the present study, 77 mRNAs were positively or negatively associated with HuR expression levels. However, the majority of these mRNAs were not reported to be regulated by HuR in other types of cells, indicating the presence of a cell type- or organ-specific regulatory network. Calcium retinal protein 2 (calretinin, calb2), a calcium binding protein, is mainly expressed in the nervous system, ovary, adrenal glands and

testis (36). This protein functions as a sensor and buffer of intracellular Ca^{2+} to prevent Ca^{2+} overloading. Increasing evidence indicates that calretinin is involved in multiple physiological processes by regulating Ca^{2+} (37). Ca^{2+} has been identified as a messenger that coordinates endoplasmic reticulum (ER)-mitochondrial interactions that regulate apoptosis (38). Induction of ER stress has been reported to enhance chemotherapy sensitization (39). Therefore, the regulation of Ca^{2+} release is tightly controlled and a number of Ca^{2+}-binding proteins, such as calretinin, may function downstream of ER Ca^{2+} release to modulate apoptosis or other cell functions. NLRP10 is involved in the innate immune response by contributing to proinflammatory cytokine release in response to invasive bacterial infection (40) and contributes to T-cell-mediated inflammatory responses in the skin. SERPINE1 is required for stimulation of keratinocyte migration during cutaneous injury repair (41) and is involved in cellular and replicative senescence (42). These mRNAs may be novel and direct targets of HuR for cosmetic treatments and to combat skin injury.

Skin aging is a slow and complex process subjected to intrinsic alterations at the cellular, molecular and genetic levels and by exposure to extrinsic factors (43). Aging affects all layers of the skin; in particular, the underlying epidermis and dermis undergo numerous cellular and molecular changes due to aging (44). The skin, as an external organ, is inevitably exposed to radiation that induces various skin reactions. Ionizing radiation is widely used in military, industrial, agricultural, medical and pollution treatments. Ionizing radiation causes both direct and indirect damage to the cells (45). DNA is the major cellular target of ionizing radiation and can be damaged directly by ionizing radiation, resulting in DNA double-strand breaks, or indirectly through the generation of ROS (46). HuR facilitates radiation resistance in triple-negative breast cancer (TNBC) by protecting against radiation-induced DNA damage (47). Silencing HuR results in radiosensitization of TNBC cells due to enhanced ROS accumulation along with inhibition of the thioredoxin reductase system (47).

The results of RIP-Seq analyses identified 14 mRNAs that preferentially interacted with HuR after ionizing radiation. A number of these genes are known to participate in certain key cellular processes, including proliferation, apoptosis, immune response and metastasis. For example, ENDOCAN is a novel human endothelial cell-specific molecule mainly expressed in endothelial cells in various tissues (48) and is expressed and secreted by vascular endothelial cells, including the skin (49). ENDOCAN is known to be involved in the development of vascular tissue in health and disease (50). IL-33 has been reported to be constitutively expressed in the nuclei of endothelial and epithelial cells and is released into the extracellular space as an alarmin after tissue damage to alert the immune system (51). The level of alarmin IL-33 is quickly elevated in the bone marrow serum after ionizing radiation and confers radioprotection (52). Studies have shown that PID1 inhibits the phosphorylation of Akt and Erk, suggesting that PID1 may modulate the signaling pathways involved in cell proliferation and survival (53-55). Previous studies have shown that CLCA2 is a stress-inducible gene and is strongly upregulated by p53 in response to cell detachment, DNA damage and other stressors (56,57). CLCA2 is a novel UVB target gene that may serve a role in epidermal differentiation and UV-dependent skin malignancies (58). These findings suggest that these 14 HuR-interacting mRNAs may contribute to enhanced regeneration and damage repair potential following irradiation. Therefore, HuR is likely to modulate skin cell radiosensitivity through complex mechanisms.

In order for HuR to exert its effects, it must dimerize prior to binding its targets. Thus, targeting of HuR may offer the ability to modulate a broad range of HuR-mediated effects, by interfering with the actions of a single target. HUR served a positive role in modulating proliferation, senescence and radiosensitivity of skin cells and modulated downstream mRNAs implicated in multiple pathways in skin cells, providing a new therapeutic strategy for cosmetic treatments and to combat skin injury.

Acknowledgements

Not applicable.

Funding

The present study supported by the National Natural Science Foundation of China (grant nos. 32071238, 82073477 and 31770909), Natural Science Foundation of Sichuan Province (grant no. 2020YJ0194), Natural Science Project of Chengdu Medical College (grant nos. CYZ19-31 and CYZZD20-01) and Young Talent Program of China National Nuclear Corporation.

Availability of data and materials

The datasets generated and/or analyzed during the current study are available in the Gene Expression Omnibus repository, https://www.ncbi.nlm.nih.gov/geo/query/acc.cgi?Acc=GSE161811 and GSE111823.

Authors' contributions

DY and SZ confirm the authenticity of all the raw data. DY and SZ conceived and designed the study. DY, KF and ZJ carried out the molecular biology studies. DY, YF and TY drafted the manuscript and figures, prepared the samples for RNA-seq and carried out the senescence studies. SZ, YS and JZ performed the statistical analysis. DY and SZ edited the manuscript. All authors read and approved the final manuscript.

Ethics approval and consent to participate

Not applicable.

Patient consent for publication

Not applicable.

Competing interests

The authors declare that they have no competing interests.

References

1. Pope SD and Medzhitov R: Emerging principles of gene expression programs and their regulation. Mol Cell 71: 389-397, 2018.
2. Zerdes I, Matikas A, Bergh J, Rassidakis G and Foukakis: Genetic, transcriptional and post-translational regulation of the programmed death protein ligand 1 in cancer: Biology and clinical correlations. Oncogene 37: 4639-4661, 2018.
3. Zhang Q and Cao X: Epigenetic regulation of the innate immune response to infection. Nat Rev Immunol 19: 417-432, 2019.
4. Hartman ML and Czyz M: MITF in melanoma: Mechanisms behind its expression and activity. Cell Mol Life Sci 72: 1249-1260, 2015.
5. Grammatikakis I, Abdelmohsen K and Gorospe M: Posttranslational control of HuR function. Wiley Interdiscip Rev RNA 8: e1372, 2017.
6. Moutal A, White KA, Chefdeville A, Laufmann RN, Vitiello PF, Feinstein D, Weimer JM and Khanna R: Dysregulation of CRMP2 post-translational modifications drive its pathological functions. Mol Neurobiol 56: 6736-6755, 2019.
7. Buuh ZY, Lyu Z and Wang RE: Interrogating the roles of post-translational modifications of non-histone proteins. J Med Chem 61: 3239-3252, 2018.
8. Schultz CW, Preet R, Dhir T, Dixon DA and Brody JR: Understanding and targeting the disease-related RNA binding protein human antigen R (HuR). Wiley Interdiscip Rev RNA 11: e1581, 2020.
9. Wang X, Zhou X, Li G, Zhang Y, Wu Y and Song W: Modifications and trafficking of APP in the pathogenesis of Alzheimer's disease. Front Mol Neurosci 10: 294, 2017.
10. Han ZJ, Feng YH, Gu BH, Li YM and Chen H: The post-translational modification, SUMOylation, and cancer. Int J Oncol 52: 1081-1094, 2018.
11. Estevez A, Zhu D, Blankenship C and Jiang J: Molecular interrogation to crack the case of O-GlcNAc. Chemistry 26: 12086-12100, 2020.
12. Zhou H, Rao Y, Sun Q, Liu Y, Zhou X, Chen Y and Chen J: MiR-4458/human antigen R (HuR) modulates PBX3 mRNA stability in melanoma tumorigenesis. Arch Dermatol Res 312: 665-673, 2020.
13. Andrade D, Mehta M, Griffith J, Oh S, Corbin J, Babu A, De S, Chen A, Zhao YD, Husain S, *et al*: HuR reduces radiation-induced DNA damage by enhancing expression of ARID1A. Cancers 11: 2014, 2019.
14. Xu X, Song C, Chen Z, Yu CX, Wang Y, Tang Y and Luo J: Downregulation of HuR inhibits the progression of esophageal cancer through interleukin-18. Cancer Res Treat 50: 71-87, 2018.
15. Mostaan LV, Tabari A, Amiri P, Ashtiani MK, Mahdkhah A, Yazdani N, Khaniki M, Tabari A, Tavakkoly-Bazzaz J and Amoli MM: Survivin gene polymorphism association with tongue squamous cell carcinoma. Genet Test Mol Biomarkers 17: 74-77, 2013.
16. Srikantan S and Gorospe M: HuR function in disease. Front Biosci (Landmark Ed) 17: 189-205, 2012.
17. Hinman MN and Lou H: Diverse molecular functions of Hu proteins. Cell Mol Life Sci 65: 3168-3181, 2008.
18. Wang J, Wang B, Bi J and Zhang C: Cytoplasmic HuR expression correlates with angiogenesis, lymphangiogenesis, and poor outcome in lung cancer. Med Oncol 28 (Suppl 1): S577-S585, 2011.
19. Zhou Y, Chang R, Ji W, Wang N, Qi M, Xu Y, Guo J and Zhan L: Loss of scribble promotes snail translation through translocation of HuR and enhances cancer drug resistance. J Biol Chem 291: 291-302, 2016.
20. To KK, Leung WW and Ng SS: Exploiting a novel miR-519c-HuR-ABCG2 regulatory pathway to overcome chemoresistance in colorectal cancer. Exp Cell Res 338: 222-231, 2015.
21. Zhang S, Wang W, Gu Q, Xue J, Cao H, Tang Y, Xu X, Cao J, Zhou J, Wu J and Ding WQ: Protein and miRNA profiling of radiation-induced skin injury in rats: The protective role of peroxiredoxin-6 against ionizing radiation. Free Radic Biol Med 69: 96-107, 2014.
22. Wang W, Furneaux H, Cheng H, Caldwell MC, Hutter D, Liu Y, Holbrook N and Gorospe M: HuR regulates p21 mRNA stabilization by UV light. Mol Cell Biol 20: 760-769, 2000.
23. Zhang J and Bowden GT: UVB irradiation regulates Cox-2 mRNA stability through AMPK and HuR in human keratinocytes. Mol Carcinog 47: 974-983, 2008.
24. Livak KJ and Schmittgen TD: Analysis of relative gene expression data using real-time quantitative PCR and the 2(-Delta Delta C(T)) method. Methods 25: 402-408, 2001.
25. Brand RM, Epperly MW, Stottlemyer JM, Skoda EM, Gao X, Li S, Huq S, Wipf P, Kagan VE, Greenberger JS and Falo LD Jr: A topical mitochondria-targeted redox-cycling nitroxide mitigates oxidative stress-induced skin damage. J Invest Dermatol 137: 576-586, 2017.
26. Xue J, Yu C, Sheng W, Zhu W, Luo J, Zhang Q, Yang H, Cao H, Wang W, Zhou J, *et al*: The Nrf2/GCH1/BH4 axis ameliorates radiation-induced skin injury by modulating the ROS cascade. J Invest Dermatol 137: 2059-2068, 2017.
27. Bellei B and Picardo M: Premature cell senescence in human skin: Dual face in chronic acquired pigmentary disorders. Ageing Res Rev 57: 100981, 2020.
28. Toutfaire M, Bauwens E and Debacq-Chainiaux F: The impact of cellular senescence in skin ageing: A notion of mosaic and therapeutic strategies. Biochem Pharmacol 142: 1-12, 2017.
29. Lee BY, Han JA, Im JS, Morrone A, Johung K, Goodwin EC, Kleijer WJ, DiMaio D and Hwang ES: Senescence-associated beta-galactosidase is lysosomal beta- galactosidase. Aging Cell 5: 187-195, 2006.
30. Kiang JG and Olabisi AO: Radiation: A poly-traumatic hit leading to multi-organ injury. Cell Biosci 9: 25, 2019.
31. Soriano JL, Calpena AC, Souto EB and Clares B: Therapy for prevention and treatment of skin ionizing radiation damage: A review. Int J Radiat Biol 95: 537-553, 2019.
32. Wang Y, Tu W, Tang Y, Momeni A, Longaker MT and Wan DC: Prevention and treatment for radiation-induced skin injury during radiotherapy. Radiat Med Protect 1: 60-68, 2020.
33. Lal P, Cerofolini L, D'Agostino VG, Zucal C, Fuccio C, Bonomo I, Dassi E, Giuntini S, Maio DD, Vishwakarma V, *et al*: Regulation of HuR structure and function by dihydrotanshinone-I. Nucleic Acids Res 45: 9514-9527, 2017.
34. Lv Z, He K, Shi L, Shi K, Jiang T and Chen Y: Interaction between C2ORF68 and HuR in human colorectal cancer. Oncol Rep 41: 1918-1928, 2019.
35. de Silanes IL, Fan J, Yang X, Zonderman AB, Potapova O, Pizer ES and Gorospe M: Role of the RNA-binding protein HuR in colon carcinogenesis. Oncogene 22: 7146-7154, 2003.
36. Hack NJ, Wride MC, Charters KM, Kater SB and Parks TN: Developmental changes in the subcellular localization of calretinin. J Neurosci 20: RC67, 2000.
37. Schwaller B: Calretinin: From a 'simple' Ca(2+) buffer to a multifunctional protein implicated in many biological processes. Front Neuroanat 8: 3, 2014.
38. Boehning D, Patterson RL, Sedaghat L, Glebova NO, Kurosaki T and Snyder SH: Cytochrome c binds to inositol (1,4,5) trisphosphate receptors, amplifying calcium-dependent apoptosis. Nat Cell Biol 5: 1051-1061, 2003.
39. Wu Y, Fabritius M and Ip C: Chemotherapeutic sensitization by endoplasmic reticulum stress: Increasing the efficacy of taxane against prostate cancer. Cancer Biol Ther 8: 146-152, 2009.
40. Lautz K, Damm A, Menning M, Wenger J, Adam AC, Zigrino P, Kremmer E and Kufer TA: NLRP10 enhances Shigella-induced pro-inflammatory responses. Cell Microbiol 14: 1568-1583, 2012.
41. Providence KM, Higgins SP, Mullen A, Battista A, Samarakoon R, Higgins CE, Wilkins-Port CE and Higgins PJ: SERPINE1 (PAI-1) is deposited into keratinocyte migration 'trails' and required for optimal monolayer wound repair. Arch Dermatol Res 300: 303-310, 2008.
42. Kortlever RM, Higgins PJ and Bernards R: Plasminogen activator inhibitor-1 is a critical downstream target of p53 in the induction of replicative senescence. Nat Cell Biol 8: 877-884, 2006.
43. Deotto ML, Spiller A, Sernicola A and Alaibac M: Bullous pemphigoid: An immune disorder related to aging. Exp Ther Med 23: 50, 2022.
44. Bhatia E, Kumari D, Sharma S, Ahamad N and Banerjee R: Nanoparticle platforms for dermal antiaging technologies: Insights in cellular and molecular mechanisms. Wiley Interdiscip Rev Nanomed Nanobiotechnol 14: e1746, 2022.
45. Burgio E, Piscitelli P and Migliore L: Ionizing radiation and human health: Reviewing models of exposure and mechanisms of cellular damage. An epigenetic perspective. Int J Environ Res Public Health 15: 1971, 2018.
46. Barzilai A and Yamamoto K: DNA damage responses to oxidative stress. DNA Repair (Amst) 3: 1109-1115, 2004.

47. Mehta M, Basalingappa K, Griffith JN, Andrade D, Babu A, Amreddy N, Muralidharan R, Gorospe M, Herman T, Ding WQ, *et al*: HuR silencing elicits oxidative stress and DNA damage and sensitizes human triple-negative breast cancer cells to radiotherapy. Oncotarget 7: 64820-64835, 2016.
48. Suzuki H, Miyagaki T, Otobe S, Nakajima R, Oka T, Takahashi N, Kabasawa M, Suga H, Yoshizaki A, Asano Y, *et al*: Increased endocan expression in lesional skin and decreased endocan expression in sera in atopic dermatitis. J Dermatol 44: 1392-1395, 2017.
49. Zhang H, Yushkevich PA and Gee JC: Deformable registration of diffusion tensor MR images with explicit orientation optimization. Med Image Comput Comput Assist Interv 8: 172-179, 2005.
50. Roudnicky F, Poyet C, Wild P, Krampitz S, Negrini F, Huggenberger R, Rogler A, Stöhr R, Hartmann A, Provenzano M, *et al*: Endocan is upregulated on tumor vessels in invasive bladder cancer where it mediates VEGF-A-induced angiogenesis. Cancer Res 73: 1097-1106, 2013.
51. Moussion C, Ortega N and Girard JP: The IL-1-like cytokine IL-33 is constitutively expressed in the nucleus of endothelial cells and epithelial cells in vivo: A novel 'alarmin'? PLoS One 3: e3331, 2008.
52. Kim J, Kim W, Le HT, Moon UJ, Tran VG, Kim HJ, Jung S, Nguyen QT, Kim BS, Jun JB, *et al*: IL-33-induced hematopoietic stem and progenitor cell mobilization depends upon CCR2. J Immunol 193: 3792-3802, 2014.
53. Erdreich-Epstein A, Robison N, Ren X, Zhou H, Xu J, Davidson TB, Schur M, Gilles FH, Ji L, Malvar J, *et al*: PID1 (NYGGF4), a new growth-inhibitory gene in embryonal brain tumors and gliomas. Clin Cancer Res 20: 827-836, 2014.
54. Bonala S, McFarlane C, Ang J, Lim R, Lee M, Chua H, Lokireddy S, Sreekanth P, Leow MKS, Meng KC, *et al*: Pid1 induces insulin resistance in both human and mouse skeletal muscle during obesity. Mol Endocrinol 27: 1518-1535, 2013.
55. Zhang CM, Chen XH, Wang B, Liu F, Chi X, Tong ML, Ni YH, Chen RH and Guo XR: Over-expression of NYGGF4 inhibits glucose transport in 3T3-L1 adipocytes via attenuated phosphorylation of IRS-1 and Akt. Acta Pharmacol Sin 30: 120-124, 2009.
56. Walia V, Ding M, Kumar S, Nie D, Premkumar LS and Elble RC: hCLCA2 is a p53-inducible inhibitor of breast cancer cell proliferation. Cancer Res 69: 6624-6633, 2009.
57. Ramena G, Yin Y, Yu Y, Walia V and Elble RC: CLCA2 interactor EVA1 is required for mammary epithelial cell differentiation. PLoS One 11: e0147489, 2016.
58. Bart G, Hämäläinen L, Rauhala L, Salonen P, Kokkonen M, Dunlop TW, Pehkonen P, Kumlin T, Tammi MI, Pasonen-Seppänen S and Tammi RH: rClca2 is associated with epidermal differentiation and is strongly downregulated by ultraviolet radiation. Br J Dermatol 171: 376-387, 2014.